



Oyster shell element composition as a proxy for environmental studies

Paulo Sergio Cardoso da Silva^{a,*}, Wellington de Moura Farias^a,
Mauro Roger Batista Pousada Gomez^a, Jefferson Koyaishe Torrecilha^a, Flávio Roberto Rocha^a,
Marcos Antônio Scapin^a, Rafael Henrique Lazzari Garcia^a, Luis Ricardo Lopes de Simone^b,
Vanessa Simão de Amaral^c, Mouchi Vincent^d, Emmanuel Laurent^e, Paweł Rudnicki-Velasquez^f

^a Instituto de Pesquisas Energéticas e Nucleares (IPEN/CNEN-SP), Av. Prof. Lineu Prestes, 2242, CEP 05508-000, São Paulo, SP, Brazil

^b Museu de Zoologia da USP-São Paulo – SP, São Paulo, SP, Brazil

^c Universidade Federal do Espírito Santo, UFES/CEUNES, São Mateus, ES, Brazil

^d Sorbonne Université, Adaptation et Diversité en Milieu Marin, UMR 7144, Station Biologique de Roscoff, F-29680, Roscoff, France

^e Sorbonne Université, Institut des Sciences de la Terre de Paris, UMR 7193, F-75005, Paris, France

^f Department of Falsified Medicines and Medical Devices, National Medicines Institute, Chelmska 30/34 Str., 00-725, Warsaw, Poland

ARTICLE INFO

Keywords:

Crassostrea brasiliiana

Crassostrea mangle

Trace elements

Oyster shell

Environmental proxy

ABSTRACT

The use of mollusks' shell as a proxy for long-term trend prediction in the variability of coastal zones has been used as an attempt to understand the consequences that environmental changes may cause to the functioning of coastal ecosystems. This study exploited the elemental concentration, elemental ratios and mineralogy of oyster shells of the genus *Crassostrea* to infer spatial variations in the environment of the animal's growth. Modern oyster shell samples of the *Crassostrea brasiliiana* and *Crassostrea mangle* species were analyzed by neutron activation analysis, X-ray diffraction, X-ray fluorescence and Graphite Furnace Atomic Absorption Spectrometry. Data normalization by the enrichment factor relative to lanthanum (La), considered as a conservative element in seawater, and statistical multivariate analyses indicate that the elemental composition and trace element ratios differ when comparing oyster shells from different regions. The results showed that the performed analyses may be useful for the characterization of the environment in which oysters grow.

1. Introduction

Earth environments are recognized as dynamic systems over the geological eras, but there is also a consensus that contemporary environmental changes are being accelerated by anthropogenic phenomena that were started by, and are being sustained by human activities, mainly in coastal zones where the most densely populated areas are found (He and Silliman, 2019; Bini and Rossi, 2021; Agnaou et al., 2023). Understanding the long-term trends in the variability of these zones is crucial to also understand the consequences that the physicochemical changes resulting from the human impacts may cause to the functioning of coastal ecosystems. The use of biogeochemical proxies has been proven as a powerful tool for understanding how environments respond to the changes driven by both, natural and anthropogenic forces (Kim et al., 2012; Obreht et al., 2019; Binda et al., 2021).

Sclerochronology, as defined by Oschmann (2009), is the study of physical and chemical variations in the accretionary hard tissues of

organisms, and the temporal context in which they are formed. It has been applied to studies on growth patterns of different coastal and oceanic species such as corals, mollusks, and fish otoliths (McConaughy and Gillikin, 2008; Łaska et al., 2021; Peharda et al., 2021; Leclerc et al., 2023) based on the principle that the composition of the mineralized skeletons or shells of these organisms is influenced by physicochemical factors prevailing in the environment, including: the availability of elements in seawater, salinity, temperature, and mineralogy, besides being also controlled by the animal physiology (Butler and Schöne, 2017).

Minor and trace elements can be incorporated into mollusk's shell structure in substitution for calcium in the crystal lattice, as independent mineral phases or even by adsorption processes (Carriker et al., 1980; Zhao et al., 2017a,b). The formation of a carbonate shell structure involves a deposition of calcium carbonate in the form of calcite or aragonite and, in certain mollusks, both, as a polymorphic mixture (Marin et al., 2012; de Winter et al., 2021). Cations other than calcium

* Corresponding author.

E-mail address: pccsilva@ipen.br (P.S. Cardoso da Silva).

<https://doi.org/10.1016/j.jsames.2023.104749>

Received 8 October 2023; Received in revised form 17 December 2023; Accepted 17 December 2023

Available online 21 December 2023

0895-9811/© 2023 Elsevier Ltd. All rights reserved.

may also be incorporated into the shell structure. According to Cravo et al. (2007), considering only the stereo-chemical rules for the calcium carbonate crystal formation, the incorporation of these other cations into the shell structure can be easily predicted, if the biological mechanisms were not taken into account. According to these authors, magnesium and strontium are the most conservative constituents in seawater and are readily available in the forms of Mg^{2+} and Sr^{2+} ions to replace the Ca^{2+} ion, and the same can also be observed for other divalent cations, such as Fe^{2+} , Mn^{2+} , Cu^{2+} and Zn^{2+} (Stewart et al., 2021).

The capacity of bivalves to incorporate elements into their shells in amounts relative to the chemical concentrations or to the physical and biological properties of the surrounding seawater has been used in the context of paleo-climatic and paleo-environmental reconstruction (Warter and Müller, 2017; de Winter et al., 2018; Pérez et al., 2020; de Winter et al., 2020, Stringer and Prendergast, 2023.).

Most research focuses on the elements from alkaline earth metal (Mg, Sr, and Ba) incorporation into the shell due to their chemical similarity with Ca, as well as, on the study of their elemental ratios. A possible problem with the use of these ratios that several studies have pointed out is the fact that the shell concentration of such elements, although dependent on external factors, is also strongly influenced by the biological control exerted by the animal's metabolism (Freitas et al., 2016; Graniero et al., 2016; Sezer et al., 2020). Therefore, a possible approach to the problem may be the search for trace elements, or elemental ratios, whose incorporation into the carbonate matrix shells occurs due to their concentration in the aquatic environment and varies with external factors, being less dependent on the animal's metabolism. This study intended to exploit geochemical data based on the concentration of trace elements, elemental ratios and mineralogy of oyster shells of the genus *Crassostrea* from the Brazilian coast as representative of the spatial variations in the environment of the animal's growth.

2. Methods

2.1. Sampling

A total of 55 oyster shells of the species *Crassostrea mangle* (Amaral and Simone, 2014) and *Crassostrea brasiliana* (Lamarck, 1819) were obtained from the collection of the University of São Paulo Zoology Museum (MZUSP), from oyster breeding farms, and from local commerce on beaches of different localities, from Rio Grande do Sul to Ceará states, covering an area ranging from the South to the North of the Brazilian coast. The location of the samples collection is shown in Fig. 1.

The removal of surface contaminants was carried out with the aid of a Dremel 4000 micro grinding machine using fiberglass reinforced cutting discs, a silicon carbide tip, and sandpaper. Then, the samples were immersed in a 4% hydrochloric acid solution for 1 min. After acid treatment, samples were washed with ultra-pure water until the solution of the washing liquid reached pH 6.5 and oven dried at 100 °C. For the analysis, a whole piece of approximately 3 cm from the umbo, without any layer separation was collected, to integrate concentration variations over the oyster growing period, and manually ground in an agate mortar and the samples were passed through an aluminum sieve with nylon mesh at a particle size of 150 μm .

2.2. X-ray diffraction

The determination of the mineralogical composition of the carbonate crystalline structure of the *C. mangle* and *C. brasiliana* shell was performed by X-ray diffraction. To perform the procedure, six specimens were randomly selected. A 3 kW Bruker D8 Advance diffractometer was used, equipped with a Cu- α radiation tube ($\lambda = 1.54056 \text{ \AA}$) and a scintillation detector. The samples were inserted into the diffractometer and analyzed from an angle of 20–80 θ . The resulting diffractograms were compared with the EVA database software to identify the crystal



Fig. 1. Brazil's map, indicating the approximately geographical coordinates of the states, and corresponding number of specimens (in parentheses) analyzed in the second set of samples.

structures of the samples.

2.3. Neutron activation analysis

Instrumental Neutron Activation Analysis (INAA), a non-destructive and multi-elemental analysis method was used. This technique consists of bombarding a given material followed by measuring the induced radioactivity. In general, the activation of the elements present in the sample is done with thermal neutrons and the resulting radioactivity is measured using spectrometry of the gamma rays emitted by the formed radioisotope (Greenberg et al., 2011). The concentration is determined by comparing the peak areas, obtained in the gamma spectrum of the irradiated sample with the gamma spectrum of reference materials irradiated together with the samples, in the same conditions.

Two irradiation schemes, short (20 s) and long irradiations (8 h) were used. The short one was used to determine the abundance of Mg. The long scheme was used for the determination of As, Br, K, La, Na, Nd, Sb, Sm, Tb, U, Yb, Ba, Ca, Ce, Co, Cr, Cs, Eu, Fe, Hf, Lu, Rb, Sb, Sc, Se, Ta, Th, Zn, and Zr. Approximately 70 mg and 100 mg of the powdered samples were analyzed in the short and long irradiation stages, respectively. Sample and reference materials were packed in previously cleaned polyethylene bags and irradiated in the IEA-R1 research reactor at the Instituto de Pesquisa Energéticas e Nucleares, IPEN, under a neutron flux of $1-5 \times 10^{12} \text{ n cm}^{-2} \text{ s}^{-1}$. The reference materials used were Rhyolite, Glass Mountain RGM-2, NIST 1646a (Estuarine Sediment), and filter paper strips in which standard solutions (SPEX Certiprep) were pipetted in precisely determined concentrations. The gamma-ray spectra were obtained using an EG&G ORTEC counting system (high-resolution solid-state Ge detector, type POP TOP, Model, 20190) with a resolution of 1.9 keV for the 1332 keV peak of ^{60}Co . This detector was coupled to an EG&G ORTEC ACE8K card and associated electronics. Spectrum analysis was performed using the VISPECT2 software in TURBOBASIC language.

2.4. X-ray fluorescence

To determine the elements Si, P, S, Cl and Sr, wavelength dispersive X-ray fluorescence (WDXRF) was used. Approximately 1 g of the powder sample was compacted in a hydraulic press using a pressure of 20 MPa s^{-1} on a boric acid base ($\pm 1.5 \text{ g of H}_3\text{BO}_3 \text{ p.a.}$), previously compacted with 50 MPa s^{-1} . At the end of this process, double-layer pressed tablets with $25.00 \pm 0.01 \text{ mm}$ in diameter and $5.0 \pm 0.2 \text{ mm}$ in total thickness were obtained. The spectrometer used was a WDXRF, Rigaku Co., model RIX 3000. The operating parameters were: X-ray tube with Rh anode (50 kV \times 50 mA), 20 mm collimator; scintillation detector (NaI/T) for $Z > 20$ and proportional flow counter for $Z \leq 20$. Quantitative determination was performed using the Fundamental Parameters method, using the 2 theta Scan mode, available in the software coupled to the spectrometer. The evaluation of the methodology, in terms of precision and accuracy, was performed using statistical tests according to DOQ-CGCRE-008 (INMETRO, 2011), applied in replicates of seven measurements in the certified reference material (SRM) 1400, Bone Ashes, from NIST.

2.5. Graphite furnace atomic absorption spectrometry

The concentration of Pb in the samples was determined by Graphite Furnace Atomic Absorption Spectrometry (GF AAS). Approximately 300 mg of pulverized shell samples were weighed. Then, 2 mL of concentrated HNO_3 were added for dissolution. The samples were filtered on filter paper with a glass funnel and placed in Teflon tubes. The tube volume was made up to 25 mL with ultrapure water. The reference material Mixed Polish Herbs (INCT-MPH-2) was used to validate the method. The digested samples, together with the reference materials were analyzed in a PerkinElmer model AAnalyst 800 GF AAS equipment.

2.6. Statistical analysis

Hierarchical Cluster Analysis (HCA), or clustering, with the purpose of separating objects into groups for reducing the dimensionality of data, allowing thousands of pieces of information to be represented by a few groups of similar behaviors and for detecting samples with anomalous behavior in the dataset (Giacomino et al., 2011); and Factor Analysis (FA) were used to better visualize and interpret the differences between the variables and examine the relationships that may exist between the samples (Barbosa et al., 2019). Using FA samples that present anomalous behavior are easily identified with the projection of the data.

With the objective of emphasizing the chemical behavior of the elements in the environment and minimizing the variations resulting from the biological control of the animal, the Enrichment Factor (EF), generally applied to soil and sediment, approach was used. It consists in establishing a mathematical relationship between the concentration of a given element and the concentration of a conservative element, which represents a certain mineral fraction in the sample (Sun et al., 2018; Arisekar et al., 2021). This conservative element must be particularly stable, characterized by low longitudinal mobility in the environment and not be influenced by anthropogenic contributions (Barbieri, 2016; Bern et al., 2019). Elements of natural origin that are structurally combined with one or more mineral phases associated with metals can be considered conservative, however the decision as to the most appropriate element must be made after careful examination of the prevailing conditions.

If the normalized EF model is followed, a correlation between the ratio of the concentration of a given element and the concentration of the conservative element, normalized by the same ratio in a reference environment, must be established highlighting the enrichment process. Works that apply the EF concept seeks to highlight anthropic influences (Vineethkumar et al., 2020). In the present work, this concept will be applied to highlight processes related to elemental absorption controlled by the animal metabolism, separating them from those whose incorporation into the oyster shell depends mostly on the natural abiotic factors and, therefore, characterize the oyster growth environment.

The selected normalization technique was the calculation of the Enrichment Factor - EF (El-Sorogy et al., 2016; Thiombane et al., 2019), and the concentration of elements in seawater (Bruland, 1983) was used as a comparison standard and La as a conservative element due to its ability to form strong complexes with carbonate and was determined in more than 80% of the samples. Enrichment factor and normalization, especially improved by principal component analysis, could reveal the trace elements sources and how they relate (Bern et al., 2019). The enrichment factor was calculated according to Equation (1):

$$EF = \frac{\left(\frac{E_S}{La_S}\right)}{\left(\frac{E_{SW}}{La_{SW}}\right)} \quad (1)$$

being:

- E_S = concentration of element in the sample;
- La_S = lanthanum concentration in the sample;
- E_{SW} = concentration of the element in seawater;
- La_{SW} = lanthanum concentration in seawater.

3. Results

For the validation of the analytical method, the limit of quantification (LQ) for INAA, GF AAS, and XRF, is presented in Table 1 and the results obtained for the reference material INCT-MPH-2 (Mixed Polish Herbs) are presented in Table 2. Although of a different matrix, the reference material INCT-MPH-2 was chosen for quality control due to the fact that it presents concentrations for the trace elements of interest of the same order of magnitude that found in shall carbonate. The E_n -

Table 1

Limit of Quantification (LQ) values, in $\mu\text{g g}^{-1}$, for INAA and GF AAS techniques, obtained for the elements in the reference material INCT-MPH-2, and for FRX technique, obtained for the elements in the NIST SRM 1400.

| Neutron Activation Analysis ($\mu\text{g g}^{-1}$) | | | |
|---|--------|---------|--------|
| Element | LQ | Element | LQ |
| As | 0.12 | Na | 0.07 |
| Ba | 7 | Nd | 1.1 |
| Br | 0.14 | Rb | 0.6 |
| Ce | 0.17 | Sb | 0.009 |
| Co | 0.019 | Sc | 0.0015 |
| Cr | 0.21 | Se | 0.13 |
| Cs | 0.027 | Sm | 0.005 |
| Eu | 0.007 | Ta | 0.022 |
| Fe | 0.0011 | Tb | 0.015 |
| Hf | 0.007 | Th | 0.018 |
| La | 0.04 | Yb | 0.04 |
| Lu | 0.005 | Zn | 0.4 |
| Mg | 77 | Zr | 9 |
| Mn | 0.4 | U | 0.05 |
| X Ray Fluorescence (%) | | | |
| Ca | 1.12 | Al | 11 |
| P | 0.67 | Sr | 2 |
| Si | 0.02 | | |
| Graphite Furnace Atomic Absorption ($\mu\text{g g}^{-1}$) | | | |
| Pb | 0.054 | | |

Table 2

Results obtained for the MR INCT-MPH-2 used for the verification and validation of the INAA and GF AAS analysis, presenting the certified value, the determined value, the relative standard deviation (RSD), the relative error (RE) and the E_n -Score results.

| Element | INCT-MPH-2 | | | | | | |
|-----------------|------------|-------------|---------|--------------|---------|--------|--------------|
| | Cert. V. | $\pm\sigma$ | Det. V. | $\pm\sigma$ | RSD (%) | RE (%) | E_n -score |
| As | 0.191 | ± 0.023 | 0.283 | ± 0.002 | 18 | -48 | 0.6 |
| Ba | 32.5 | ± 2.5 | 39 | ± 4 | 17 | -21 | 0.8 |
| Br | 7.71 | ± 0.61 | 13.08 | ± 0.05 | 29 | -70 | 0.5 |
| Ce | 1.12 | ± 0.1 | 0.941 | ± 0.005 | 21 | 16 | 1 |
| Co | 0.21 | ± 0.025 | 0.2676 | ± 0.0006 | 4 | -27 | 0.7 |
| Cr | 1.69 | ± 0.13 | 2.24 | ± 0.01 | 21 | -33 | 0.7 |
| Cs | 0.076 | ± 0.13 | 0.0871 | ± 0.0007 | 13 | -15 | -0.6 |
| Eu | 0.016 | ± 0.002 | 0.0263 | ± 0.0001 | 28 | -64 | 0.5 |
| Fe ^a | 0.046 | / | 0.0553 | ± 0.0001 | 6 | - | - |
| Hf | 0.236 | ± 0.02 | 0.2135 | ± 0.0004 | 16 | 10 | 1 |
| La | 0.571 | ± 0.046 | 0.548 | ± 0.003 | 20 | 4 | 1 |
| Lu | 0.009 | ± 0.002 | 0.0076 | ± 0.0001 | 25 | 15 | 0.9 |
| Mg | 0.292 | ± 0.018 | 0.30 | ± 0.02 | 0.02 | -1 | 0.9 |
| Mn | 191 | ± 12 | 201 | ± 2 | 10 | -5 | -0.8 |
| Na ^a | 350 | / | 363 | ± 4 | 7 | - | - |
| Nd | 0.457 | ± 0.091 | 0.50 | ± 0.03 | 15 | -9 | 0.7 |
| Pb | 2.16 | ± 0.23 | 1.53 | / | 2 | 29 | - |
| Rb | 10.7 | ± 0.7 | 12.2 | ± 0.2 | 6 | -14 | 0.8 |
| Sb | 0.066 | ± 0.009 | 0.0617 | ± 0.0007 | 14 | 7 | 0.9 |
| Sc | 0.123 | ± 0.009 | 0.1299 | ± 0.0001 | 4 | -6 | 0.9 |
| Sm | 0.094 | ± 0.008 | 0.0808 | ± 0.0003 | 16 | 14 | 1.1 |
| Ta | 0.019 | ± 0.002 | 0.0166 | ± 0.0003 | 40 | 13 | 1 |
| Tb | 0.014 | ± 0.001 | 0.0134 | ± 0.0002 | 37 | 4 | 1 |
| Th | 0.154 | ± 0.001 | 0.152 | ± 0.001 | 21 | 2 | 1 |
| U ^a | 0.049 | / | 0.0942 | ± 0.0002 | 20 | -92 | - |
| Yb | 0.053 | ± 0.007 | 0.0473 | ± 0.0001 | 19 | 11 | 1 |
| Zn | 33.5 | ± 2.1 | 33 | ± 2 | 6 | 1 | 0.9 |

^a No certified value; Cert. V. = certified value; Det. V. = determined value; RSD = Relative standard deviation; RE = Relative error.

score criterion (INMETRO, 2011) was used to assess the accuracy achieved in the elementary determinations. A result is considered satisfactory when E_n values are between -1 and 1, ensuring that an individual result of the control sample (reference material) is within the 95% confidence interval of the true or accepted value.

3.1. Elemental abundances in *Crassostrea brasiliana* and *Crassostrea mangle* oyster shell samples

The results obtained for elemental abundances of *C. brasiliana* and *C. mangle* shell samples are summarized in Table 3 with the statistical descriptive analysis and Supplementary Material 1 shows the statistical descriptive according to the state of samples collection. In Table 3, the number of valid results is also shown, i.e., number of determinations above the limit of quantification according to the employed analytical technique. Among the determined elements, the relative standard deviation (RSD) for all the measurements was below 10% for Ca and Sr; between 10 and 50% for Cs, P, S, Sb, Se; between 50 and 100% for As, Br, Ce, Co, Eu, Fe, La, Lu, Mg, Mn, Na, Nd, Pb, Si, Sm, Ta, Th, Yb, Zr and higher than 100% for Ba, Cl, Cr, Hf, Rb, Sc, Tb, U, Zn.

3.2. Mineralogical composition of *Crassostrea brasiliana* and *Crassostrea mangle* shell samples

In Fig. 3, the diffractograms for two samples from the South (Paraná and Santa Catarina), Southeast (Rio de Janeiro and Espírito Santo) and Northeast (Bahia and Rio Grande do Norte) coastal regions in Brazil are shown. The diffractograms of the samples were compared to reference diffractograms, showing a predominant composition of calcite and the absence of aragonite in the carbonate shells.

3.3. Multivariate analysis of the elemental concentrations in *Crassostrea brasiliana* and *Crassostrea mangle* shell samples using non-normalized data

The first approach to interpret the results was to apply the multivariate statistical analyses to the abundance values. Only the elements that were determined in 70% or more of samples were considered for this purpose.

The observed variability of the data was verified with Factor Analysis using normalized Vimax rotation and a loading factor greater than 0.7 (Fig. 4). Five factors were extracted contributing a total of 62.45% of the explained variance. The first factor is composed by the elements Mg, Si, and S with weak significant negative correlation with Ca. Factor 2 is composed of the elements P, Na, Br, and Cl. Factor 3 is due to Mn, and Factors 4 and 5 are composed of the metals La, Zn and Fe. Pearson correlation coefficients results for this analysis are shown in supplementary material 2.

3.4. Multivariate analysis of the elemental concentrations in *Crassostrea brasiliana* and *Crassostrea mangle* shell samples using the normalized data by the enrichment factor

Fig. 5 shows the loading factors obtained by applying the FA for the normalized values obtained by the EF. Factor 1 accounts for 78.45% and Factor 2, composed by Br, Mn, and Cr, accounts only for 7.87% of the variability, and does not significantly contribute to the data variation. This value is much higher than that obtained in the analysis of the non-transformed data, indicating that using the normalized EF values is more effective in the identification of patterns based on the absorption distribution of the elements in the shell matrix.

4. Discussion

4.1. Elemental abundances in *Crassostrea brasiliana* and *Crassostrea mangle* oyster shell samples

Statistical descriptive analysis indicated that the skewness results showed a negative value only for the elements Ca and P indicating that the distribution curves for these elements have a slight tendency to the left, due to a greater number of results with values below the average. The elements Cl, S, Si, Sr, Fe, Br, Co, Cr, Cs, Eu, La, Mg, Mn, Na, Pb, Sc,

Table 3

Descriptive analysis of the results obtained for each element showing the number of valid results (N), Mean, lowest value (minimum), highest value (maximum), relative standard deviation (RSD), relative error (RE), skewness and kurtosis.

| Element | N | Mean | Minimum | Maximum | RSD (%) | RE (%) | Skewness | Kurtosis |
|-----------------------------|----|--------|---------|---------|---------|--------|----------|----------|
| As ($\mu\text{g.g}^{-1}$) | 3 | 0.2 | 0.1 | 0.3 | 58 | 0.06 | 1 | |
| Ba ($\mu\text{g.g}^{-1}$) | 27 | 5 | 1 | 26 | 112 | 1 | 3 | 8 |
| Br ($\mu\text{g.g}^{-1}$) | 48 | 8 | 1 | 35 | 82 | 1 | 2 | 8 |
| Ca (%) | 51 | 38 | 36 | 40 | 2 | 0.1 | -1 | 0.2 |
| Ce ($\mu\text{g.g}^{-1}$) | 26 | 0.30 | 0.02 | 0.77 | 79 | 0.05 | 1 | -1 |
| Cl (%) | 50 | 0.14 | 0.01 | 0.63 | 103 | 0.02 | 2 | 2 |
| Co ($\mu\text{g.g}^{-1}$) | 50 | 0.082 | 0.006 | 0.299 | 79 | 0.01 | 2 | 3 |
| Cr ($\mu\text{g.g}^{-1}$) | 44 | 0.72 | 0.07 | 3.30 | 114 | 0.1 | 2 | 2 |
| Cs ($\mu\text{g.g}^{-1}$) | 41 | 0.024 | 0.006 | 0.046 | 40 | 0.001 | 0.2 | -0.1 |
| Eu ($\mu\text{g.g}^{-1}$) | 44 | 0.0076 | 0.0009 | 0.0180 | 52 | 0.001 | 1 | 0.2 |
| Fe (%) | 37 | 0.0029 | 0.0004 | 0.0097 | 83 | 0.0004 | 2 | 2 |
| Hf ($\mu\text{g.g}^{-1}$) | 19 | 0.026 | 0.003 | 0.092 | 110 | 0.007 | 2 | 2 |
| La ($\mu\text{g.g}^{-1}$) | 44 | 0.120 | 0.005 | 0.383 | 78 | 0.01 | 1 | 0.3 |
| Lu ($\mu\text{g.g}^{-1}$) | 11 | 0.003 | 0.001 | 0.011 | 93 | 0.001 | 2 | 5 |
| Mg ($\mu\text{g.g}^{-1}$) | 47 | 2785 | 784 | 8882 | 59 | 241 | 2 | 6 |
| Mn ($\mu\text{g.g}^{-1}$) | 50 | 28 | 3 | 91 | 74 | 3 | 1 | 1 |
| Na ($\mu\text{g.g}^{-1}$) | 50 | 3830 | 1403 | 13,134 | 52 | 282 | 3 | 10 |
| Nd ($\mu\text{g.g}^{-1}$) | 31 | 0.79 | 0.05 | 4.22 | 93 | 0.1 | 4 | 16 |
| P (%) | 50 | 0.033 | 0.008 | 0.053 | 33 | 0.002 | -0.3 | -0.1 |
| Pb ($\mu\text{g.g}^{-1}$) | 49 | 0.9 | 0.1 | 2.6 | 62 | 0.1 | 1 | 1 |
| Rb ($\mu\text{g.g}^{-1}$) | 17 | 0.8 | 0.1 | 5.5 | 153 | 0.3 | 3 | 13 |
| S (%) | 50 | 0.14 | 0.07 | 0.24 | 33 | 0.006 | 1 | -1 |
| Sb ($\mu\text{g.g}^{-1}$) | 9 | 0.03 | 0.02 | 0.05 | 36 | 0.003 | 1 | 1 |
| Sc ($\mu\text{g.g}^{-1}$) | 47 | 0.0068 | 0.0004 | 0.0304 | 106 | 0.001 | 2 | 4 |
| Se ($\mu\text{g.g}^{-1}$) | 33 | 0.10 | 0.03 | 0.18 | 46 | 0.008 | 0.3 | -1 |
| Si (%) | 50 | 0.017 | 0.005 | 0.050 | 63 | 0.002 | 1 | 2 |
| Sm ($\mu\text{g.g}^{-1}$) | 29 | 0.016 | 0.001 | 0.051 | 77 | 0.002 | 1 | 1 |
| Sr (%) | 51 | 0.04 | 0.03 | 0.05 | 10 | 0.001 | 0.3 | 0.3 |
| Ta ($\mu\text{g.g}^{-1}$) | 8 | 0.017 | 0.005 | 0.055 | 100 | 0.006 | 2 | 4 |
| Tb ($\mu\text{g.g}^{-1}$) | 9 | 0.017 | 0.002 | 0.068 | 126 | 0.007 | 2 | 5 |
| Th ($\mu\text{g.g}^{-1}$) | 20 | 0.017 | 0.003 | 0.050 | 66 | 0.003 | 2 | 3 |
| U ($\mu\text{g.g}^{-1}$) | 11 | 0.20 | 0.01 | 0.82 | 120 | 0.07 | 2 | 4 |
| Yb ($\mu\text{g.g}^{-1}$) | 14 | 0.033 | 0.006 | 0.109 | 86 | 0.01 | 1 | 3 |
| Zn ($\mu\text{g.g}^{-1}$) | 46 | 4 | 1 | 15 | 103 | 0.6 | 2 | 3 |
| Zr ($\mu\text{g.g}^{-1}$) | 21 | 7 | 1 | 17 | 73 | 1 | 1 | -1 |

Zn showed positive values for skewness, with a larger distribution of measurement above the mean. Values closer to zero for the elements Cs, Sr and Se indicate a good homogeneity in the results. The results of kurtosis of the elements Cs, Ce, P, S, Se and Zr had negative values indicating a greater distribution along the normal curve. The elements As, Ba, Br, Ca, Cl, Co, Cr, Cs, Eu, Fe, Hf, La, Lu, Mg, Mn, Na, Nd, P, Pb, Rb, Sb, Sc, Si, Sm, Sr, Ta, Tb, Th, U, Yb, Zn, presented positive kurtosis values, ranging from 0.2 for Ca and Eu, which indicates little asymmetry up to 16 for Nd, indicating that the normal distribution curve of this element has a concentration of results more dispersed in relation to the average.

Fig. 2 shows the mean values and standard deviation of the results obtained in the shell samples, sorted by the Brazilian state in which the collection was carried out (Supplementary material 1). The elements were separated by their respective orders of magnitude. The results for calcium showed a variation from 35.7 to 39.5% of mass fraction in the composition of the shells, with a mean value of 38.2%. Although consisting basically of calcium carbonate, the average concentration of this element in bivalve shells is around 37.9% (Onuma et al., 1979), in agreement with the values found in this study.

4.2. Mineralogical composition of *Crassostrea brasiliana* and *Crassostrea mangle* shell samples

Rahman et al. (2013) concluded that the calcite formation takes place even when the physical-chemical environment in sea water should favor aragonite formation, evidencing that the process control is driven by animal biology, therefore affecting the absorption capacity of trace elements (Du et al., 2011). Therefore, the variations in the elemental concentrations observed for the samples analyzed in this study should not be related to the mineralogy of the shell, as all of them possess a

calcite structure.

4.3. Multivariate analysis of the elemental concentrations in *Crassostrea brasiliana* and *Crassostrea mangle* shell samples using non-normalized data

It was observed, as shown in Fig. 4, that among the elements with chemical behavior like Ca, only Mg showed a significant weak negative correlation with it, probably related to the competition between the ions of these elements. Mg/Ca ratios have been investigated in mollusk shells as a temperature proxy, as seasonal fluctuations appear to exist along the growth direction of the shell (Mouchi et al., 2013, 2018; Durham et al., 2017). A competition between these elements is therefore expected. Strontium and Pb, which are also referred to as calcium analogue elements, did not present significant correlation with it. In studies of mollusk shell composition, the element Sr and the Sr/Ca ratio are investigated in the attempt to correlate these values with temperature (Marali et al., 2017; Geeza et al., 2019). Similarly, the Mn/Ca ratio is used as an indicator of redox processes, depending on the availability of the Mn^{2+} ion (Zhao et al., 2017a,b). However, no correlation was also found between Ca and Sr or Mn with the non-normalized data in this study.

The extraction of phosphorus with weak significant positive correlations with Br, Cl, and Na (Fig. 4) may indicate some correlation between salinity and primary productivity as shown by van der Molen and Perissinotto (2011). In this analysis, few correlations were observed between the metallic elements, with each other or with calcium.

The HCA was applied to verify if using non-normalized data, the samples could be separated according to their provenance. The result is shown in supplementary material 3 and it was verified that, at a cut in 60% of similarity, 5 groups with low similarity were obtained. In this

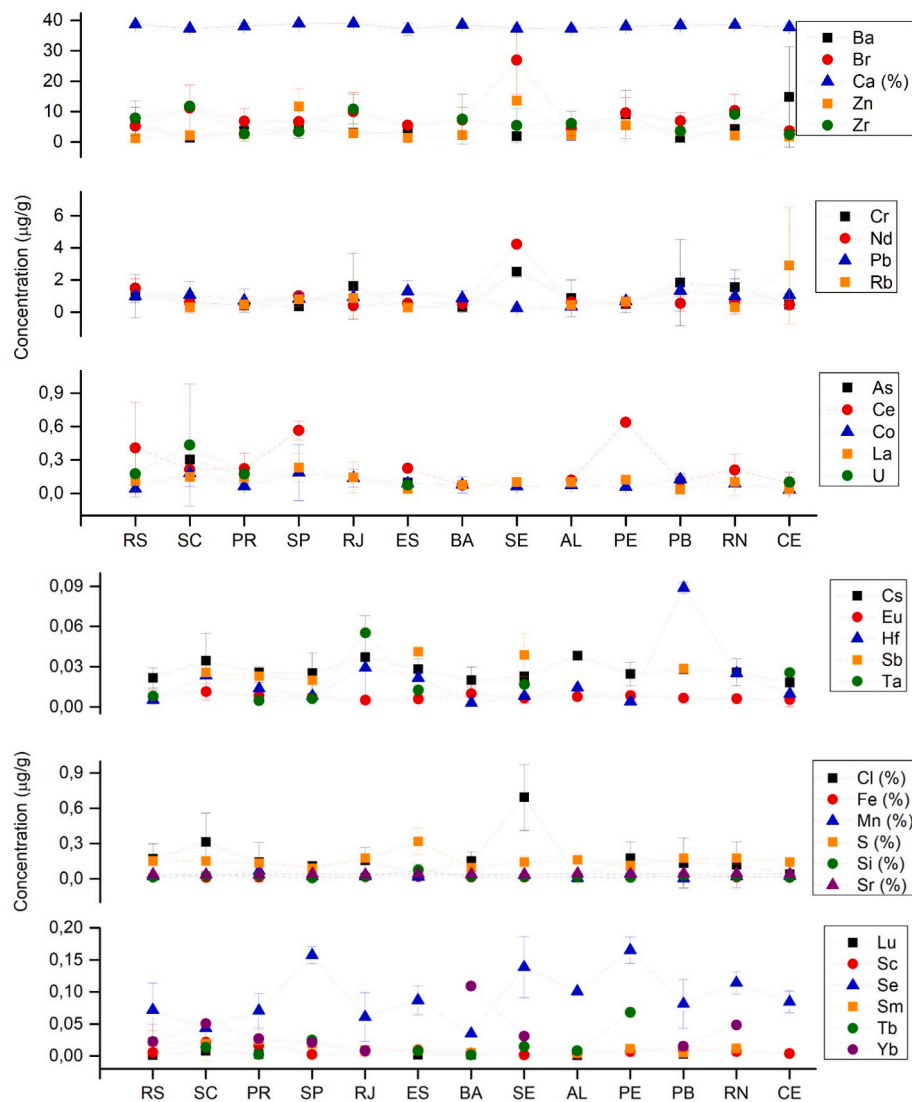


Fig. 2. Mean abundances (in $\mu\text{g g}^{-1}$, except where indicated %) and standard deviation of the determined elements, organized by collection state: South (RS, SC, PR), Southeast (SP, RJ, ES), and Northeast (BA, SE, AL, PE, PB, RN, CE).

case, a good similarity between the samples cannot be asserted, according to their collection region or their species.

4.4. Multivariate analysis of the elemental concentrations in *Crassostrea brasiliana* and *Crassostrea mangle* shell samples using the normalized data by the enrichment factor

Considering the values obtained from the EF normalization, significant positive correlations (shown in supplementary material 4) can be observed between Ca and almost all the elements considered with emphasis for the perfect correlation with Sr (1.00). Exceptions were observed only for the correlation between Ca and Br, Cr and Mn. Although weak, the highest correlation value presented by Mn was with Eu (0.44), another element also influenced by the redox conditions of the environment.

The strong correlation between Ca and P (0.99) may be related to the fact that phosphates and sulfates contribute to form the basis for the formation and growth of the shell crystal structure matrix, which may explain the strong correlation also observed between calcium and sulfur (0.97) (Wheeler, 1992) and P and S (0.94). Iron is a limiting element of primary production in coastal environments, with a great affinity for phosphate in that environment (Testa et al., 2002), which may justify

the behavior of the correlation observed with the elements P, S and Ca itself.

It can also be observed that Si, although a limiting element of the biochemical behavior of oysters (Enright et al., 1986), showed strong correlations with most of the determined elements, and did not show any correlation with Br and Mn. In the case of the latter, this is probably because Si concentrations in the oyster's growth environment is strongly influenced by the adjacent phytoplankton community that also controls Mn availability (Spalt et al., 2020). In turn, the elements Mg, Sr and Pb, which have chemical behavior like calcium, have remarkably similar correlations with this element.

In the attempt to verify if the concentrations of elements normalized by EF could show any pattern among the samples, the HCA was applied and the resulting dendrogram is shown in Fig. 6. It can be observed that the formation of better-characterized groups occurred given that, at a cut in 20% of distance, four main groups were obtained.

The first group is formed exclusively by the outlier sample PB-2, of the *C. mangle* species. The second, formed by six samples, mixing the two analyzed species, *C. mangle* and *C. brasiliana*, being three of each species. In the third group, the predominant presence of samples of the species *C. brasiliana* is observed except for samples SE-2 and RJ-2, while in the fourth group, practically all samples of the species *C. mangle* are found,

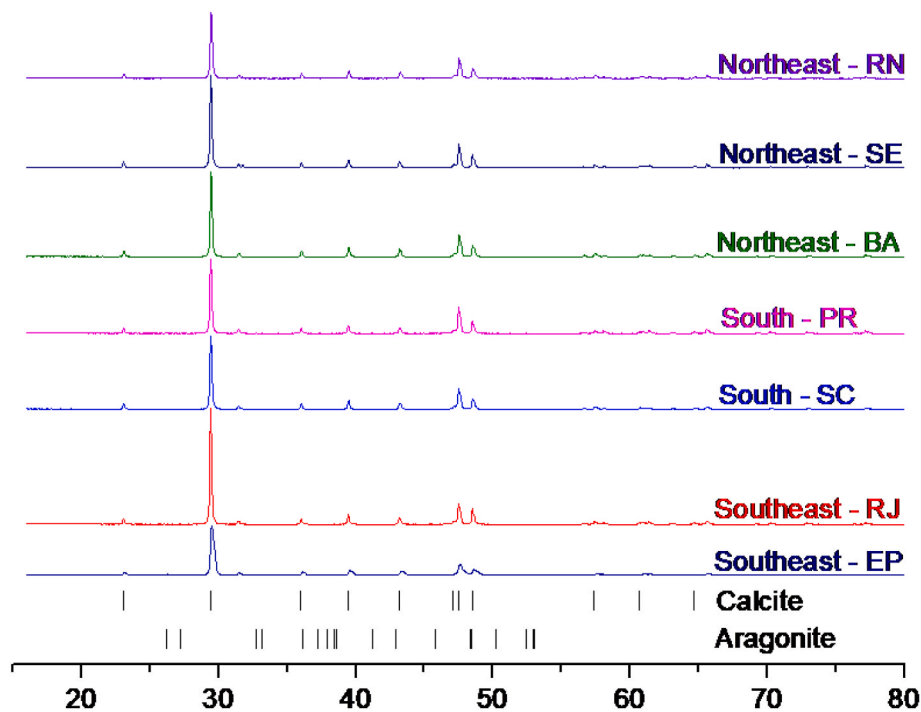


Fig. 3. Diffractograms of samples representing the South (Paraná and Santa Catarina), Southeast (Rio de Janeiro and Espírito Santo), and Northeast (Bahia and Rio Grande do Norte) regions of Brazilian coast, obtained by X-Ray diffraction analysis.

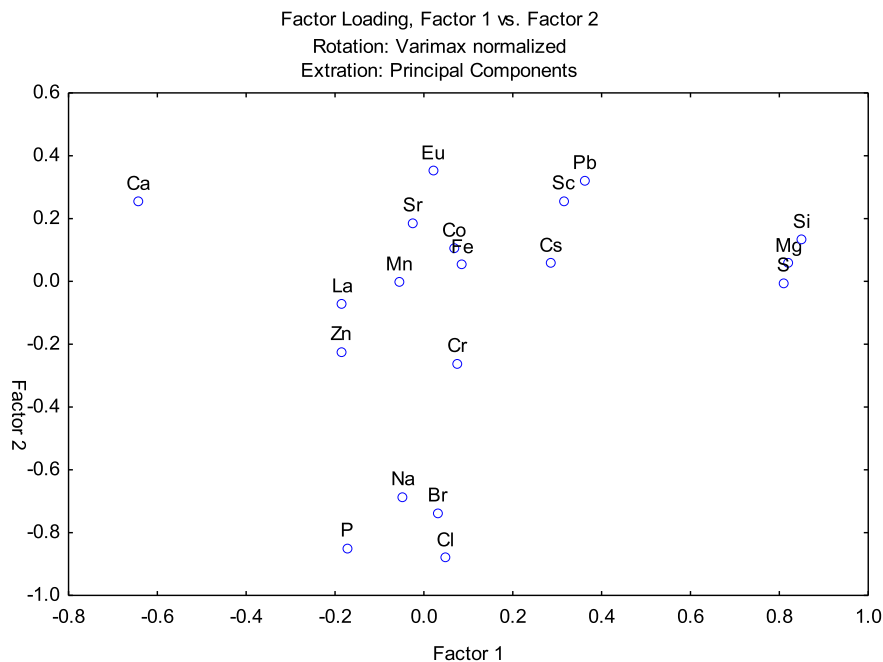


Fig. 4. Loading factors 1 × 2 for non-normalized data.

except for samples BA-2 and BA-5. The *C. mangle* species grows in mangrove environments while *C. brasiliana* can grow in environments that vary from estuarine to marine, with greater salinity (Amaral and Simone, 2014). Therefore, this result can be considered more successful as a good separation was obtained due to the *Crassostrea* oyster shell chemical composition, which varies according to the growth environment.

The formation of a group of samples that did not group with their

respective species (group 2), as well as the presence of *C. mangle* among the samples of the *C. brasiliana* group and vice versa could not be explained with the data collected till this point and more studies are needed to explain the observed inconsistencies.

5. Conclusion

Major, minor and trace elements were determined in shell samples

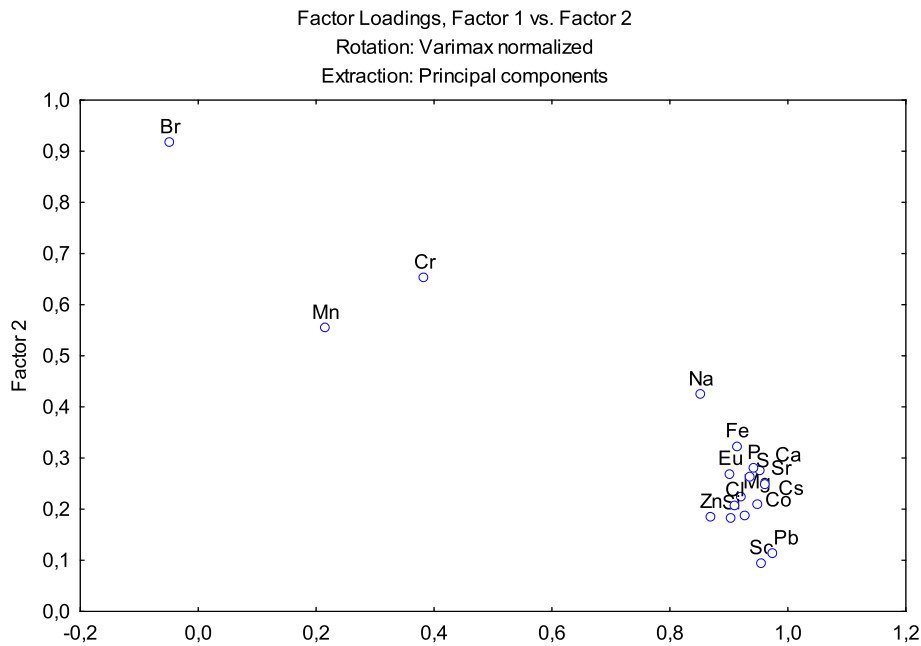


Fig. 5. Loading factors 1 × 2 for the data normalized by the enrichment factor.

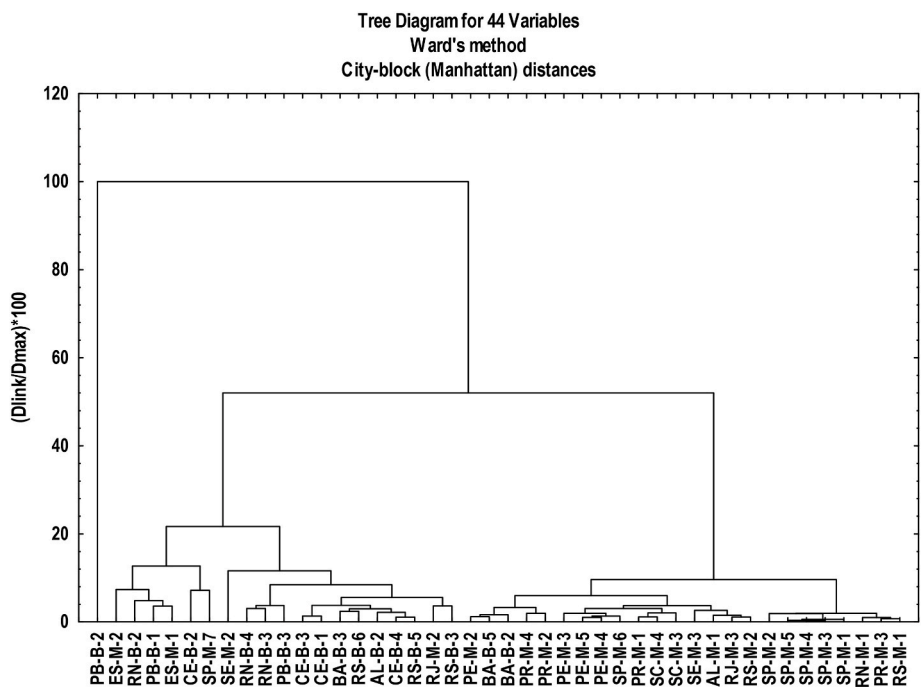


Fig. 6. Dendrogram obtained for the normalized data by the EF. Letter M indicates that the sample belongs to the species *Crassostrea mangle* and letter B, *Crassostrea brasiliiana*.

collected from different parts of the Brazilian coast. The obtained results using the non-normalized data indicated that the main factors responsible for the observed variations are Mg, Si and S, which present a negative correlation with calcium. Negative correlations were also observed for the characteristic elements indicators of salinity (Na, Cl and Br) and P, typically a primary productive indicator. However, all observed correlations can be considered weak and thus it is not possible to observe a characterization as a function of the collection environment.

The use of EF to normalize the data, otherwise, allowed for the explanation of approximately 78% of the observed variance and its

application to hierarchical cluster analysis allowed the formation of two groups composed mainly of samples from each of the analyzed species, comprising 37 out of the 44 samples considered in the analysis. A group formed by six samples did not show adequate separation between species or collection site and one sample showed an outlier behavior. Since the species *C. mangle* is characteristic of estuarine regions while *C. brasiliiana* grows in environments that vary from estuarine to marine, it can be considered that the groups formed were separated according to the chemical characteristics of their growth environment.

Thus, the application of the EF concept to elementary concentrations of oyster shell samples can be a promising indicator of environmental

variation. The refinement of the data, expanding the number of analyzed samples, obtaining a greater number of elements and adding the characterization of the collection sites can contribute to the application of elemental carbonate structures of the shells as environmental indicators.

CRedit authorship contribution statement

Paulo Sergio Cardoso da Silva: Writing - review & editing, Writing - original draft, Supervision, Methodology, Data curation, Conceptualization. **Wellington de Moura Farias:** Formal analysis. **Mauro Roger Batista Pousada Gomez:** Formal analysis. **Jefferson Koyaishe Torrecilha:** Formal analysis. **Flávio Roberto Rocha:** Conceptualization. **Marcos Antônio Scapin:** Methodology, Formal analysis. **Rafael Henrique Lazzari Garcia:** Formal analysis. **Luis Ricardo Lopes de Simone:** Data curation, Conceptualization. **Vanessa Simão de Amaral:** Investigation, Data curation, Conceptualization. **Mouchi Vincent:** Writing - review & editing, Writing - original draft, Data curation. **Emmanuel Laurent:** Writing - review & editing, Writing - original draft, Data curation. **Paweł Rudnicki-Velasquez:** Data curation.

Declaration of competing interest

The authors declare that they have no known competing financial interests or personal relationships that could have appeared to influence the work reported in this paper.

Data availability

Data will be made available on request.

Acknowledgments

Authors thank the Fundação de Amparo à Pesquisa do Estado de São Paulo, FAPESP, and the Conselho Nacional de Desenvolvimento Científico e Tecnológico, CNPq, for the scholarships grants. Special thanks, in memoriam, to Wellington Moura Farias, dedicated master degree student and friend.

Appendix A. Supplementary data

Supplementary data to this article can be found online at <https://doi.org/10.1016/j.jsames.2023.104749>.

References

- Agnaou, M., El Mourabit, Y., Nadir, M., Oualid, J.A., Elmchichi, K., Sahla, K., Lefrere, L., Banaoui, A., Alla, A.A., 2023. Integrated biomarker responses in the mollusk, *patella vulgata*: assessing aquatic pollution in agadir bay, South Morocco. *Mar. Pollut. Bull.* 196, 115660.
- Amaral, V.S., Simone, L.R., 2014. Revision of genus *Crassostrea* (Bivalvia: ostreidae) of Brazil. *J. Mar. Biol. Assoc. U. K.* 94 (4), 811–836.
- Arisekar, U., Shakila, R.J., Shalini, R., Sivaraman, B., Jeyasekaran, G., Malini, N.A.H., 2021. Heavy metal concentration in reef-associated surface sediments, Hare Island, Gulf of Mannar Marine Biosphere Reserve (southeast coast of India): the first report on pollution load and biological hazard assessment using geochemical normalization factors and hazard indices. *Mar. Pollut. Bull.* 162, 111838.
- Barbieri, M., 2016. The importance of enrichment factor (EF) and geoaccumulation index (Igeo) to evaluate the soil contamination. *J. Geol. Geophys.* 5 (1), 1000237.
- Barbosa, I.S., Brito, G.B., Santos, G.L., Santos, L.N., Teixeira, L.S.G., Araujo, R.G.O., Korn, M.G.A., 2019. Multivariate data analysis of trace elements in bivalve molluscs: characterization and food safety evaluation. *Food Chem.* 273, 64–70.
- Bern, C.R., Walton-Day, K., Naftz, D., 2019. Improved enrichment factor calculations through principal component analysis: examples from soils near breccia pipe uranium mines, Arizona, USA. *Environ. Pollut.* 248, 90–100.
- Binda, G., Di Iorio, A., Monticelli, D., 2021. The what, how, why, and when of dendrochemistry: (paleo)environmental information from the chemical analysis of tree rings. *Sci. Total Environ.* 758, 143672.
- Bini, M., Rossi, V., 2021. Climate change and anthropogenic impact on coastal environments. *Water* 13, 1182.
- Bruland, K.W., 1983. In: Riley, J.P., Chester, R. (Eds.), *Trace Elements in Sea Water*. III Chemical Oceanography, vol. 8. Academic Press, London, pp. 157–220.

- Butler, P.G., Schöne, B.R., 2017. New research in the methods and applications of sclerochronology. *Palaeogeogr. Palaeoclimatol. Palaeoecol.* 465, 295–299. Part B.
- Carriker, M.R., Palmer, R.E., Sick, L.V., Johnson, C.C., 1980. Interaction of mineral elements in sea water and shell of oysters (*Crassostrea virginica* Gmelin) cultured in controlled and natural systems. *J. Exp. Mar. Biol. Ecol.* 46, 279–296.
- Cravo, A., Foster, P., Almeida, C., Company, R., Cosson, R.P., Bebian, M.J., 2007. Metals in the shell of *Bathymodiolus azoricus* from a hydrothermal vent site on the Mid-Atlantic Ridge. *Environ. Int.* 33, 609–615.
- de Winter, N.J., Dämmer, L.K., Falkenroth, M., Reichart, G., Moretti, S., Martínez-García, A., Höche, N., Schöne, B.R., Rodiouchkina, K., Goderis, S., Vanhaecke, F., van Leeuwen, S.M., Ziegler, M., 2021. Multi-isotopic and trace element evidence against different formation pathways for oyster microstructures. *Geochem. Cosmochim. Acta* 308, 326–352.
- de Winter, N.J., Goderis, S., Malderen, S.J.M.V., Sinnesael, M., Vansteenberge, S., Snoeck, C., Belza, J., Vanhaecke, F., Claeys, P., 2020. Subdaily-scale chemical variability in a *Torresites* *Sanchezii* rudist shell: implications for rudist paleobiology and the cretaceous day-night cycle. *Paleoceanogr. Paleoclimatol.* 35, e2019PA003723.
- de Winter, N.J., Vellekoop, J., Vorrsselmans, R., Golreihan, A., Soete, J., Petersen, S.V., Meyer, K.W., Casadio, S., Speijer, R.P., Claeys, P., 2018. An assessment of latest Cretaceous *Pycnodonte vesicularis* (Lamarck, 1806) shells as records for palaeoseasonality: a multi-proxy investigation. *Clim. Past* 14, 725–749.
- Du, Y., Lian, F., Zhu, L., 2011. Biosorption of divalent Pb, Cd and Zn on aragonite and calcite mollusk shells. *Environ. Pollut.* 159, 1763–1768.
- Durham, S.R., Gillikin, D.P., Goodwin, D.H., Dieltz, G.P., 2017. Rapid determination of oyster lifespans and growth rates using LA-ICP-MS line scans of shell Mg/Ca ratios. *Palaeogeogr. Palaeoclimatol. Palaeoecol.* 485, 201–209.
- El-Sorogy, A.S., Youssef, M., Al-Kahtany, K., Al-Otaiby, N., 2016. Assessment of arsenic in coastal sediments, seawaters and molluscs in the tarut island, arabian gulf, Saudi arabia. *J. Afr. Earth Sci.* 113, 65–72.
- Enright, C.T., Newkirk, G.F., Craigie, J.S., Castell, J.D., 1986. Growth of juvenile *Ostrea edulis* L. fed *Chaetoceros gracilis* Schütt of varied chemical composition. *J. Exp. Mar. Biol. Ecol.* 96 (1), 15–26.
- Freitas, P.S., Clarke, L.J., Kennedy, H., Richardson, C.A., 2016. Manganese in the shell of the bivalve *Mytilus edulis*: seawater Mn or physiological control? *Geochem. Cosmochim. Acta* 194, 266–278.
- Geeza, T.J., Gillikin, D.P., Goodwin, D.H., Evans, S.D., Watters, T., Warner, N.R., 2019. Controls on magnesium, manganese, strontium, and barium concentrations recorded in freshwater mussel shells from Ohio. *Chem. Geol.* 526, 142–152.
- Giacomino, A., Abollino, O., Malandrino, M., Mentasti, E., 2011. The role of chemometrics in single and sequential extraction assays: a Review. Part II. Cluster analysis, multiple linear regression, mixture resolution, experimental design and other techniques. *Anal. Chim. Acta* 688 (2), 122–139.
- Graniero, L.E., Surge, D., Gillikin, D.P., Briz i Godino, I., Álvarez, M., 2016. Assessing elemental ratios as a paleotemperature proxy in the calcite shells of patelloid limpets. *Palaeogeogr. Palaeoclimatol. Palaeoecol.* 465, 386–395.
- Greenberg, R.R., Bode, P., de Nadai Fernandes, E.A., 2011. Neutron activation analysis: a primary method of measurement. *Spectrochim. Acta B Atom Spectrosc.* 66 (3–4), 193–241.
- He, Q., Silliman, B.R., 2019. Climate change, human impacts, and coastal ecosystems in the anthropocene. *Curr. Biol.* 29 (19), R1021–R1035.
- INMETRO, 2011. *Orientação sobre validação de métodos analíticos. DOQ-CGCRE-008: revision 04-Jul/2011. Rio de Janeiro, 2011 (in Portuguese)*. Available at: www.inmetro.gov.br/Sidoq/Arquivos/Cgcre/DOQ/DOQ-Cgcre-8.04.pdf. Accessed on: 21 Aug. 2020.
- Kim, K.J., Zolitschka, B., Jull, A.J.T., Ohlendorf, C., Haberzettl, T., Matsuzaki, H., 2012. Tracing environmental change in southern Patagonia using beryllium isotopes, Laguna Potrok Aike, Argentina. *Quat. Geochronol.* 9, 27–33.
- Laska, W., Rodríguez-Tovar, F.J., Uchman, A., 2021. Bioerosion structures from the pliocene of the agua amarga subbasin (almería, SE Spain): palaeoecological and palaeoenvironmental implications. *Palaeogeogr. Palaeoclimatol. Palaeoecol.* 562, 110071.
- Leclerc, N., Kuehn, S., Clark, T., Burchell, M., Coupland, G., Schöne, B., 2023. Investigation of seasonal settlement and clam harvest pressure in the sechelt inlet system, British Columbia, Canada, through sclerochronology and stable oxygen isotope analysis. *Environ. Archaeol.* 1–12.
- Marali, S., Schone, B.R., Mertz-kraus, R., Grifin, S.M., Wanamaker, A.D., Butler, P.G., Jochum, K.P., 2017. Reproducibility of trace element time-series (Na/Ca, Mg/Ca, Mn/Ca, Sr/Ca, and Ba/Ca) within and between specimens of the bivalve *Arctica islandica* – a LA-ICP-MS line scan study. *Palaeogeogr. Palaeoclimatol. Palaeoecol.* 484, 109–128.
- Marin, F., Le Roy, N., Marie, B., 2012. The formation and mineralization of mollusk shells. *Front. Biosci.* 4, 1099–1125.
- McConnaughey, T.A., Gillikin, D.P., 2008. Carbon isotopes in mollusk shell carbonates. *Geo Mar. Lett.* 28, 287–299.
- Mouchi, V., de Rafélis, M., Lartaud, F., Fialin, M., Verrecchia, E., 2013. Chemical labeling of oyster shells used for time-calibrated high resolution Mg/Ca ratios: a tool for past estimation of seasonal temperature variations. *Palaeogeogr. Palaeoclimatol. Palaeoecol.* 373, 66–74.
- Mouchi, V., Briard, J., Gaillot, S., Argant, T., Forest, V., Emmanuel, L., 2018. Reconstructing environments of collection site from archaeological bivalve shells: case study from oysters (Lyon, France). *J. Archaeol. Sci.: Reports* 21, 1225–1235.
- Obrecht, I., Zeeden, C., Hambach, U., Veres, D., Marković, S.B., Lehmkühf, F., 2019. A critical reevaluation of palaeoclimate proxy records from loess in the Carpathian Basin. *Earth Sci. Rev.* 190, 498–520.

- Onuma, N., Masuda, F., Hirano, M., Wada, K., 1979. Crystal structure control on trace element partition in molluscan shell formation. *Geochem. J.* 13 (4), 187–189.
- Oschmann, W., 2009. Sclerochronology: editorial. *Int. J. Earth Sci.* 98, 1–2.
- Peharda, M., Schöne, B.R., Black, B.A., Corrège, T., 2021. Advances of sclerochronology research in the last decade. *Palaeogeogr. Palaeoclimatol. Palaeoecol.* 570, 110371.
- Pérez, A.E., Batres, D.A., Rocchetta, I., Eppis, M.R., Bianchi, M.L., Luquet, C.M., 2020. Paleoenvironmental reconstruction using stable isotopes and trace elements from archaeological freshwater bivalve shell fragments in Northwest Patagonia, Argentina. *Quat. Int.* 547, 22–32.
- Rahman, M.A., Halfar, J., Shinjo, R., 2013. X-Ray Diffraction is a promising tool to characterize coral skeletons. *Adv. Mater. Phys. Chem.* 3 (1A), 120–125.
- Sezer, N., Kılıç, Ö., Sıkdokur, E., Çayır, A., Belivermiş, M., 2020. Impacts of Elevated pCO₂ on Mediterranean Mussel (*Mytilus galloprovincialis*): Metal Bioaccumulation, Physiological and Cellular Parameters. *Marine Environmental Research.*, 104987
- Spalt, N., Murgulet, D., Abdulla, H., 2020. Spatial variation and availability of nutrients at an oyster reef in relation to submarine groundwater discharge. *Sci. Total Environ.* 710, 136283.
- Stringer, C.A., Prendergast, A.L., 2023. Freshwater mollusc sclerochronology: trends, challenges, and future directions. *Earth Sci. Rev.* 247, 104621.
- Stewart, B.D., Jenkins, S.R., Boig, C., Sinfield, C., Kennington, K., Brand, A.R., Lart, W., Kröger, R., 2021. Metal pollution as a potential threat to shell strength and survival in marine bivalves. *Sci. Total Environ.* 755 (1), 143019.
- Sun, X., Fan, D., Liu, M., Tian, Y., Pang, Y., Liao, H., 2018. Source identification, geochemical normalization and influence factors of heavy metals in Yangtze River Estuary sediment. *Environ. Pollut.* 241, 938–949.
- Testa, J.M., Charette, M.A., Sholkovitz, E.R., Allen, M.C., Rago, A., Herbold, C.W., 2002. Dissolved iron cycling in the subterranean estuary of a coastal bay: waquoit Bay, Massachusetts. *Biol. Bull.* 203 (2), 255–256.
- Thiombane, M., Di Bonito, M., Albanese, S., Zuzolo, D., Lima, A., De Vivo, B., 2019. Geogenic versus anthropogenic behavior and geochemical footprint of Al, Na, K and P in the Campania region (Southern Italy) soils through compositional data analysis and enrichment factor. *Geoderma* 335, 12–26.
- van der Molen, J.S., Perissinotto, R., 2011. Microalgal productivity in an estuarine lake during a drought cycle: the St. Lucia Estuary, South Africa. *Estuarine, Coastal and Shelf Science* 92 (1), 1–9.
- Vineethkumar, V., Sayooj, V.V., Shimod, K.P., Prakash, V., 2020. Estimation of pollution indices and hazard evaluation from trace elements concentration in coastal sediments of Kerala, Southwest Coast of India. *Bull. Natl. Res. Cent.* 44, 198.
- Warter, V., Müller, W., 2017. Daily growth and tidal rhythms in Miocene and modern giant clams revealed via ultra-high resolution LA-ICPMS analysis - a novel methodological approach towards improved sclerochemistry. *Palaeogeogr. Palaeoclimatol. Palaeoecol.* 465, 362–375.
- Wheeler, A.P., 1992. Phosphoproteins of oyster (*Crassostrea virginica*) shell organic matrix. In: Suga, S., Watabe, N. (Eds.), *Hard Tissue Mineralization and Demineralization*. Springer, Tokyo.
- Zhao, L., Walliser, E.O., Mertz-Kraus, R., Schöne, B.R., 2017a. Unionid shells (*Hyriopsis cumingii*) record manganese cycling at the sediment-water interface in a shallow eutrophic lake in China (Lake Taihu). *Palaeogeogr. Palaeoclimatol. Palaeoecol.* 484, 97–108.
- Zhao, L., Schöne, B.R., Mertz-Kraus, R., 2017b. Delineating the role of calcium in shell formation and elemental composition of *Corbicula fluminea* (Bivalvia). *Hydrobiologia* 790, 259–272.